LA-UR -90-4427

Received by OSTI

JAN 0 8 1991

LA-UR--90-4427

DE91 005936

TITLE: THREE DIMENSIONAL, TRANSIENT NATURAL CONVECTION IN INCLINED WELLBORES

AUTHOR(S): D. M. McEligot, Westinghouse Elect. Corp.
D. A. Denbow, Software Ag.
H. D. Murphy, EES-DOT

SUBMITTED TO: Nat'l Heat Transfer Conf., ASME,
Minneapolis, MN
July 28-31, 1991

DISCLAIMER

Los Alamos National Laboratory
Los Alamos, New Mexico 87545

FORM NO. 836 R4
ST. NO. 2629 5/81

DISCLAIMER

THREE-DIMENSIONAL, TRANSIENT NATURAL CONVECTION IN INCLINED WELLBORES

by

Donald M. McEligot,* David A. Denbow,** and Hugh D. Murphy+

ABSTRACT

To simulate natural convection flow patterns in directionally drilled wellbores, experiments and analyses were conducted for a circular tube with length to diameter (L/D) ratio of 36 at angles of 0°, 20°, and 35° from the vertical. The tube was heated at the bottom and cooled at the top, and the insulation was adjusted so that approximately one- to two-thirds of the power dissipated was transferred through the tube wall to the surroundings. An aqueous solution of polyvinyl alcohol was employed as the working fluid in order to obtain low Rayleigh numbers corresponding to conditions in geothermal wellbores. Temperature distributions were measured for the three orientations and for several heating rates to demonstrate the effects of tube angle and Rayleigh number. Comparison with measurements showed good agreement of the predicted temperature levels for the maximum inclination and slightly poorer agreement for the other limit, a vertical tube.

---

* Westinghouse Electric Corporation, Oceanic Division, Middletown, RI 02840.

** Graduate Research Assistant at Los Alamos. Presently Software AG of North America, Inc., 300 Union Blvd., Lakewood, CO 80228.

+ Staff Member, University of California, Los Alamos National Laboratory, Los Alamos, NM 87545.

NOMENCLATURE

A	area; A_c, A_{cs} cross sectional area
Bi	Biot number, h·(length)/k_{solid}
C_1	coefficient
c_p	specific heat at constant pressure
D	diameter; D_h, hydraulic diameter, $4A_{cs}/P$
$\dot{E}$	Heating rate
f	friction factor, $2g_c\tau_w/(\rho V^2)$
Fo	Fourier number, $\alpha\theta/L^2$ or $\alpha\theta/r_w^2$
g	acceleration of gravity
g_c	units conversion factor, e.g., 32.174 lbm ft/(lbf sec^2)
Gr	Grashof number, defined variously
h	convective heat-transfer coefficient
k	thermal conductivity; kinetic energy of turbulence; index in axial direction
L	length
$\dot{m}$	mass flow rate
n	number of time steps in numerical solution
Nu	Nusselt number, hD/k
P	perimeter
p	pressure
Pr	Prandtl number, $c_p\mu/k$
q	heat-transfer rate; q_G, electrical energy generation rate
q''	heat flux, q/A
R	tube radius
r	radius (pointwise)
Ra	Rayleigh number, Gr·Pr

Re Reynolds number, $\rho V D_h/\nu$

Ri Richardson number, $\omega_{BV}^2/(\frac{\partial U}{\partial z})^2$

s distance between two fluid parcels (Hines, 1971)

T temperature, absolute

t temperature, relative (e.g., °C)

U overall heat-transfer coefficient; mean velocity component in streamwise direction

V velocity

W width; mean square of vorticity fluctuations

x axial distance

y distance from wall

z axial distance (computer code); vertical distance (Hines, 1971)

GREEK LETTERS

α thermal diffusivity, $k/\rho c_p$; angle with vertical (Hines, 1971)

β volumetric coefficient of thermal expansion

ϵ dissipation of turbulent kinetic energy

θ time; potential temperature (Hess, 1959)

μ absolute viscosity

ν kinetic viscosity, μ/ρ

ρ density

τ shear stress

ϕ angle referred to vertical; azimuthal coordinate

ω_{BV} Brunt-Väisälä frequency

SUBSCRIPTS

a ambient

b bottom

c reference, cool

cr critical

E	based on energy flow rate ($\dot{E}$)
f	fluid
fd	fully developed
G	generation
h	hot
i	interface
l	loss
N	last node for region
t	top, total
u	upflow
w	wall, surface

1. INTRODUCTION

1.1. Background

The occurrence of natural convection in a wellbore can affect geothermal gradient measurements and heat-flow estimates. If particularly strong, natural convection may distort wellbore surveys and reservoir diagnostic tests. For example, convective dispersion of a tracer occurring in the injection and production wells might be falsely attributed to reservoir flow path heterogeneities. Convection is of particular importance in nonvertical wells, because theoretical results (Combarnous, 1978) indicate that stable states cannot exist, i.e., convection is always present, albeit in very weak form for low Rayleigh numbers. Ostrach (1982) made a comparable statement concerning other inclined geometries.

In general, wellbores are not exactly vertical. In the Hot Dry Rock geothermal concept shown in Fig. 1, the wellbores are purposely inclined at angles of the order of 30° from vertical in the deep regions to enhance heat production (Smith *et al.*, 1983). Even in wells not purposely inclined, unintentional deviations up to 10° from vertical are not unusual. Due to the geothermal gradient resulting in hot water underlying colder, heavier water, the water can be expected to be in a thermally unstable condition when there is no forced flow. Transport of energy and/or particles introduced as tracers then depends on whether significant natural circulation is induced and, if so, its magnitude.

Figure 2 portrays the single antisymmetric convection cell expected, in which one long circulation loop extends from bottom to top. A radially symmetric cell, which requires more energy to drive and therefore is less probable to occur, would consist of an inner core of rising (or descending) flow surrounded by an annulus of descending (or rising) flow.

The fluid temperature distribution in the more probable antisymmetric case is fully three-dimensional and depends upon the distance, x, from the bottom, the radial position, r, and the azimuthal position, ϕ. However, at any distance x, one may evaluate an average hot fluid temperature, T_h, and an average cold fluid temperature, T_c, by simply averaging over r and ϕ the temperature in the upper and lower halves of the tube, respectively. In this manner the hot side and cold side fluid temperatures can be conveniently characterized for simple hydraulics and heat-transfer computations (Donaldson, 1961). The right side of Fig. 2 shows the expected variation of T_h and T_c for a related laboratory experiment. In the absence of heat losses from the test section, the only heat transfer taking place is (1) from the heater to the fluid, (2) by exchange from the hot fluid to the cold fluid, and (3) from the

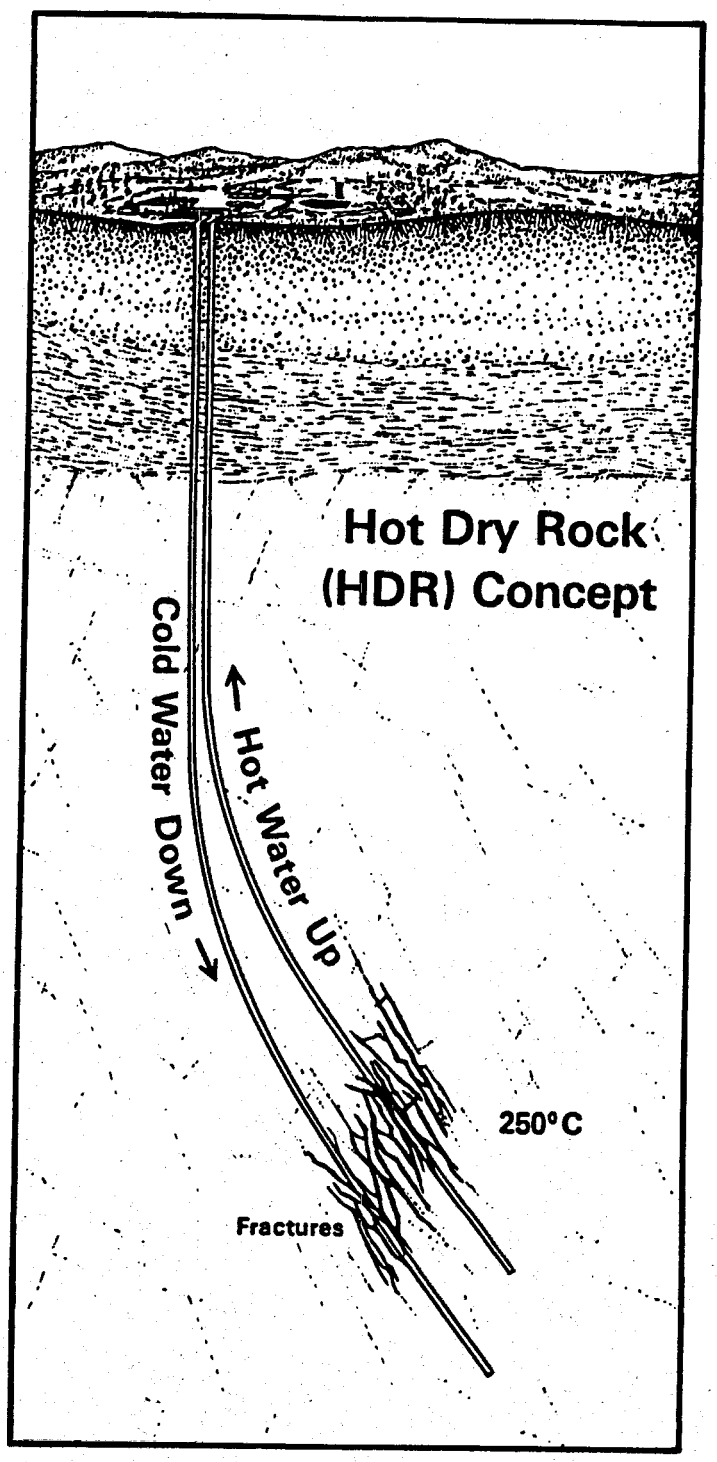

Fig. 1. Schematic diagram of hot dry rock geothermal energy reservoir.

fluid to the cooler. The temperature variation is then indicated by the two parallel lines in Fig. 2 in which the temperature difference is predicted to be constant, as demonstrated later by the idealized analysis of Section 2.

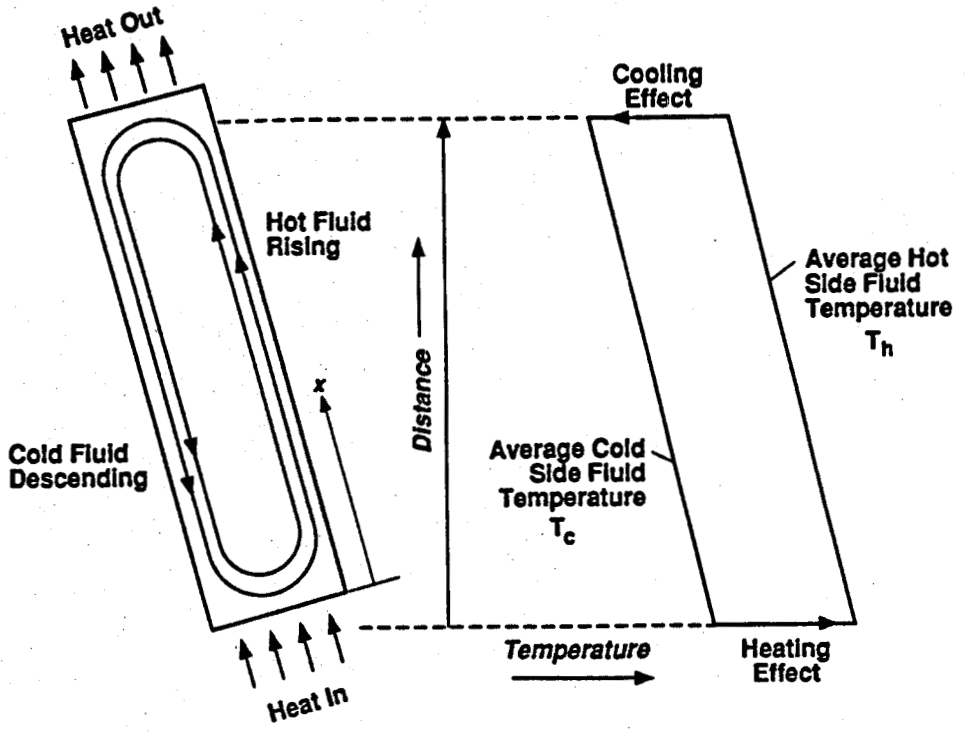

Fig. 2. Illustration of expected patterns in inclined tube heated from below.

Typical dimensions in the field experiments of the Hot Dry Rock Project are diameters of 8 in. (20 cm) and depths of 14,000 ft (4 km) (Rowley and Carden, 1982). Thus, the aspect ratios of the holes are effectively infinite. Geothermal gradients are in the range 30° to 100° C/km, with the temperature increasing with depth. A nondimensional flow parameter that characterizes the thermohydrodynamic problem is the Rayleigh number (or Grashof-Prandtl product) based on bore radius and geothermal gradient.

$$Ra = Gr \cdot Pr = \frac{\rho^2 g \beta R^4}{\mu^2} \frac{dt}{dz} \frac{c_p \mu}{k} = \frac{g \beta R^4}{\nu \alpha} \frac{dt}{dz}. \tag{1}$$

1.2. Goal and Objectives

Reliable prediction of the transport of tracers in wellbores is the ultimate goal of the overall project. The general objective is the development of understanding and predictive methods for flow patterns and temperature and velocity fields inside a long circular tube, heated below and cooled above, for angles from vertical to 35°. This report emphasizes the temperature measurements and predictions. These initial efforts concentrate on the lower end of the Rayleigh number range and on the larger inclination due to the paucity of information available in this situation and to obtain preliminary data related to thermal stability in inclined tubes.

1.3. Previous Work

For a general background concerning natural convection in enclosures and the related problem of thermosiphons, the reader is referred to the reviews of Ostrach (1982), Buchberg *et al.* (1976), Catton (1978), Japiske (1973), McEligot, Denbow, and Murphy (1990), and others. In the following discussion emphasis is on work relating to inclined tubes and long vertical tubes. Studies have concentrated on two general areas: (1) stability and identification of consequent flow patterns and (2) heat-transfer and velocity predictions for specific flow regimes.

Vertical Tubes. When a long vertical tube is filled with a fluid and subjected to a thermal gradient, such that the temperature increases with depth, the fluid will become unstable and begin to convect as soon as the gradient reaches a critical value. The fluid instability can be characterized in terms of the Rayleigh number, Eq. (1). As the buoyancy forces are increased, for example by increasing the thermal gradient, natural circulation will arise at some critical value of the Rayleigh number, Ra_{cr}. The onset of fluid motion is characterized by a cellular pattern. A single antisymmetric roll cell (fluid motion up on one side of the tube and down the opposite side) is always observed first at the onset of convection since it is the most unstable mode (Heitz and Westwater, 1971). Radial, as well as axial, temperature differences develop in the tube. Several convection patterns can be produced at elevated Rayleigh numbers up to the transition to turbulent flow. The transition to turbulent flow occurs at high Rayleigh number and is characterized by unstable flow patterns, where random plumes of warm and cold liquid rise and plunge intermittently while intermixing within the bulk fluid.

Hales (1937) analyzed convective patterns within a vertical circular cylindrical tube with a perfectly conducting wall with length much greater than its diameter. Assuming idealized boundary conditions where end effects could be neglected, he provided the critical values of Ra_{cr} for stability. Theoretical and experimental evaluations of critical Rayleigh numbers for other situations have been investigated by many authors (Ostroumov, 1952; Catton and Edwards, 1967; Diment, 1967; Gretener, 1967; Edwards, 1969; Charlson and Sani, 1970, 1971, Olson and Rosenberger, 1979).

For situations where convection has occurred, Lighthill (1953) developed methods for predicting the flow and heat transfer due to free convection in heated vertical tubes, closed at the bottom and opening into a reservoir of cool fluid at the top, the so-called open thermosiphon. Ostrach and Thornton (1958) presented an analysis of laminar natural-convection flow and heat transfer in a closed-end tube

with a linear wall temperature and large but finite length-radius ratio. Additional analytic approaches for natural convection in vertical tubes have been provided by Edwards and Catton (1969) and Donaldson (1970). Related measurements were reported by Donaldson (1970), Hasegawa, Nishikawa, and Yamagata (1963), Catton and Edwards (1967), and Verhoeven (1969).

Inclined and horizontal tubes. Flow stability in inclined tubes has not been studied frequently. Verhoeven (1969) reported observations for a pipe inclined 20° from the vertical and noted that the critical Rayleigh number for convective flow was lowered significantly. His experiments showed extreme sensitivity to inclination near the horizontal where a change of one degree in angle could cause a tenfold change in axial heat transport. Trefethen (1970) also found that the Nusselt number varied greatly for slight changes in inclination near horizontal. In related studies Hartnett *et al.* (1959), Leslie (1959), and Martin (1959) examined the effect of tilting open thermosiphons, simulating to some extent the Coriolis accelerations arising from rotation in cooling cavities inside rotor blades of gas turbines.

For heat transfer in inclined rectangular enclosures, the extensive experiments of Sherbiny *et al.* (1982) and the reviews of Buchberg *et al.* (1976) and Catton (1978) should be consulted.

When a horizontal tube is operated at different end temperatures, the resulting flow patterns show the general features observed in the present work. Kimura and Bejan (1980a and b) studied such a tube with $L/D \simeq 9$ and Rayleigh number in the range $10^8 < \mathrm{Ra}_D < 10^{10}$, and found that an upper, warm jet proceeded along the top of the cylinder toward the cold end and the lower, cold jet advanced along the bottom in the opposite direction.

1.4. Conspectus

Although heat transfer with the tube walls must be considered for geothermal and geophysical applications and is significant in the experiments conducted, it is instructive first to examine the limiting case of adiabatic inclined tubes. This situation is examined in Section 2 by means of simple, approximate analyses. Section 3 then presents the experiment and typical results. The three-dimensional transient numerical analysis is described briefly in Section 4. Section 5 compares the experimental measurements with predictions calculated for the same condition. Finally, Section 6 provides concluding remarks. Further details are available in the recent report by the authors (McEligot, Denbow, and Murphy, 1990).

2. ANALYSIS

The full description of the flow requires the solution of the Navier-Stokes equations for three velocity components plus the continuity and energy equations that are coupled to them (Schlichting, 1968). Although this system can be solved numerically by several existing computer codes (Johnson and Torok, 1985), it is instructive and useful to consider simpler approximations first.

2.1. Heat and Mass Transfer

Flow in a long inclined tube without heat loss is comparable to a closed thermosiphon loop where there is heat transfer between a riser and a downcomer, or a regenerative heat exchanger, as sketched in Fig. 3. The tube can have any cross-sectional shape that is vertically symmetric. Warm fluid rises on the upper side while the cooler fluid sinks along the lower side. This type of approach is related to "pipe flow" models applied to describe the gross features of entire geothermal areas (Einarsson, 1942; Donaldson, 1968) and solar thermosiphons (Zvirin *et al.*, 1977; Mertol *et al.*, 1981) with the exception that in the present treatment there is direct thermal communication between the riser and downcomer as in a countercurrent heat exchanger (Kays and London, 1964).

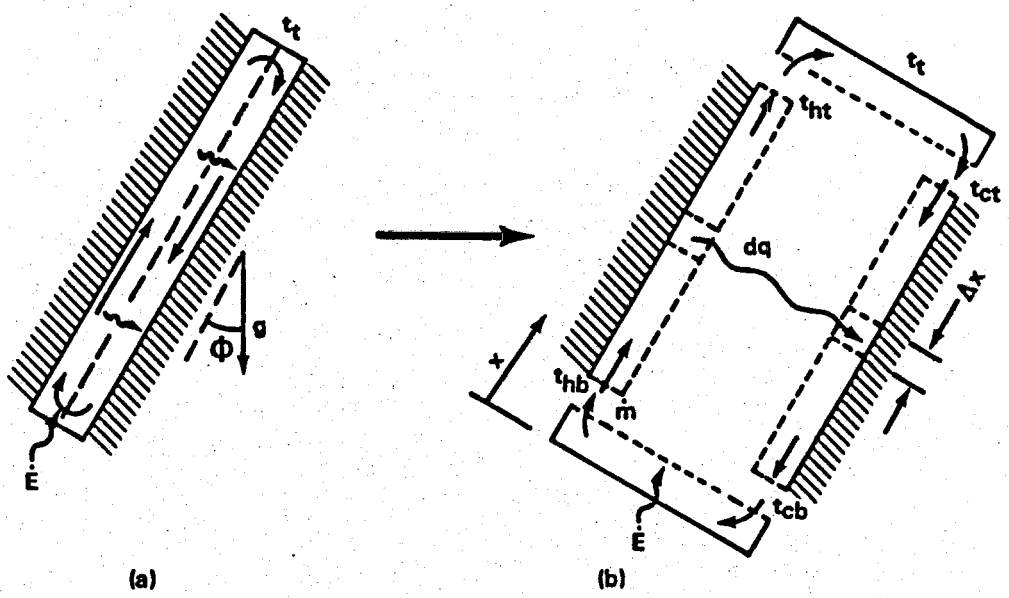

Fig. 3. Nomenclature and schematic representation of adiabatic inclined duct.

For the purpose of this part of the analysis, the following idealizations are made:

1. Laminar, steady flow.
2. The duct is sufficiently long that the flow is effectively parallel to the walls, i.e., internal boundary layer approximation.
3. Fluid properties are constant except for density (Boussinesq approximation).
4. Away from the ends, the axial pressure gradient $\frac{dp}{dx}$ is the same in both the hot and the cool leg at a given axial position, x. [This idealization is related to No. 2; if $\left(\frac{dp}{dx}\right)_h$ were significantly different from $\left(\frac{dp}{dx}\right)_c$, a nonhydrostatic gradient could form in the transverse direction and induce significant crossflow.]
5. Constant flow cross sections in both directions, up and down.
6. Tube walls are adiabatic.
7. The cross-sectional areas occupied by the upflow and downflow streams are equal.
8. In the upflow and downflow regions away from the ends, the flow is considered to be fully established.
9. Negligible streamwise conduction.

Boundary conditions are an imposed heat-transfer rate $\dot{E}$ at the lower end and a specified temperature t_t at the upper end.

Energy balances demonstrate that the temperature difference is predicted to remain constant along the tube as

$$t_h - t_c = \frac{\dot{E}}{\dot{m}c_p}. \tag{2}$$

At any section the heat-transfer rate between the two streams can be represented, as in a countercurrent heat exchanger, as

$$dq = UP\Delta x(t_h - t_c) \tag{3}$$

where P is the perimeter of the interface between the hot and cold fluid. For a circular tube with half the cross section occupied by each portion, P would be the diameter D. The overall heat-transfer

coefficient U can be deduced by considering the thermal resistance from the hot fluid to the interface and from the interface to the cooler fluid, i.e., $U = \left(\frac{1}{h_h} + \frac{1}{h_c}\right)^{-1}$. If the conditions can be considered fully established, U can be taken as constant, giving

$$\frac{dt}{dx} = -\frac{dq}{(\Delta x)\dot{m}c_p} = -\frac{UP}{\dot{m}c_p}(t_h - t_c) = constant. \tag{4}$$

That is the temperature profile is linear.

The velocity at the interface is zero by idealization No. 7, so the flow in each stream can be approximated as flow in a duct where the interface can be taken as one of the walls. Then the shear forces in either the cold or hot streams can be evaluated as

$$\tau_w P \Delta x = f \cdot \frac{\rho V^2}{2g_c} P\ \Delta x \tag{5}$$

and a comparable equation for the cold stream. For laminar flow the friction factor is of the form $f = \frac{C_1}{Re}$ where

$$Re = \frac{\rho V D_h}{\mu} = \frac{4\dot{m}}{P\mu}. \tag{6}$$

Adopting idealization No. 7, equal hot and cold flow areas, and equating the pressure gradients in the momentum equations for each stream, and substituting for τ_w from (5) and $(t_h - t_c)$ from (2) yields

$$\dot{m}^2 = \frac{4\rho^2 \beta g \dot{E}}{C_1 c_p \mu} \cdot \frac{A_{ch}^3}{P^2} \cos\phi. \tag{7}$$

Therefore, for a given situation, the mass flow rate would vary as $\sqrt{\dot{E}}$. Increasing $\dot{E}$ would increase $\dot{m}$ until the interfacial shear induced a Kelvin-Helmholtz instability and the flow would likely break up into cells and/or turbulence.

The temperature difference is

$$t_h - t_c = \frac{\dot{E}}{\dot{m}c_p} = \frac{P}{\rho A_{ch}} \sqrt{\frac{C_1}{4} \frac{\mu}{g\beta c_p} \frac{\dot{E}}{A_{ch} \cos\phi}}, \tag{8}$$

so the temperature difference between the two streams varies as $\sqrt{\dot{E}}$. The streamwise temperature gradient is independent of the energy transfer rate. It can be represented by

$$\frac{dt_c}{dx} = \frac{dt_h}{dx} = -\frac{Nu_{fd} C_1}{32} \cdot \frac{k\mu}{\rho^2 c_p \beta g} \frac{P_i P_h^3}{A_{ch}^4} \frac{1}{\cos\phi} \tag{9}$$

where Nu_{fd}, the fully developed Nusselt number for forced laminar convection in a half duct with one adiabatic wall, is constant.

The above results can be rephrased in terms of nondimensional parameters. The nondimensional temperature gradient can be written as a Rayleigh number,

$$Ra_{dt/dx} = \frac{\rho^2 g \beta D_h^4 (dt_u/dx)}{\mu^2} \cdot \frac{\mu c_p}{k} = - \frac{8 N u_{fd} C_1}{\cos \phi}, \tag{10}$$

The resulting mass flow rate can be described as a Reynolds number,

$$Re^2 = \left(\frac{\dot{m} D_h}{A_{ch} \mu}\right)^2 = \frac{1}{4C_1} \left(\frac{\rho^2 g \beta D_h^4 (\dot{E}_t''/k)}{\mu^2}\right) \left(\frac{k}{\mu c_p}\right) \left(\frac{A_{ct}}{A_{ch}}\right) \cos \phi = \frac{1}{4C_1} \frac{Gr_E}{Pr} \frac{A_{ct}}{A_{ch}} \cos \phi \tag{11}$$

where $\dot{E}_t'' = \dot{E}/A_{ct}$ is based on the total cross-sectional area instead of that of the stream.

In *summary*, for the idealizations assumed, the effects of increasing the heating rate $\dot{E}$ are

a) to increase $\dot{m}$ as $\sqrt{\dot{E}}$,

b) to increase $(t_h - t_c)$ as $\sqrt{\dot{E}}$, and

c) to leave the streamwise temperature gradient constant.

2.2. Stability

The stability of the circulating flow to disturbances in the central shear layer can be considered in terms of the gradient Richardson number,

$$Ri = \frac{\omega_{BV}^2}{\left(\frac{\partial U}{\partial z}\right)^2}, \tag{12}$$

which serves as a criterion for the onset of atmospheric turbulence (Hines, 1971). The Brunt-Väisäla frequency is defined as

$$\omega_{BV}^2 = \left(\frac{g}{\theta}\right) \cdot \left(\frac{\partial \theta}{\partial z}\right)^2, \tag{13}$$

where θ is the potential temperature (Hess, 1959). Hines (1971) shows that for nonhorizontal shear layers the stabilization criterion can be written as

$$\frac{\left(\frac{g}{\theta}\right)\left(\frac{\partial \theta}{\partial s}\right) \cos \alpha}{\left(\frac{\partial U}{\partial s}\right)^2} \leq \frac{1}{4} \tag{14}$$

where s is the axis connecting the two parcels of fluid considered and α is the angle between s and the vertical gravity vector. In our nomenclature s would be perpendicular to x and $\alpha = \left(\frac{\pi}{2}\right) - \phi$ (Fig. 3).

By approximating the velocity gradient via the difference between the bulk velocities in the two streams and taking the length scale as half the distance between the center plane and the surface, i.e.,

$$\frac{\partial U}{\partial s} \simeq \frac{2V_u}{r_w} = \frac{2\dot{m}}{(\rho A_{ch} r_w)}, \tag{15}$$

one may rephrase the Richardson number to our configuration as

$$Ri \simeq \frac{g\beta(t_h - t_c)}{r_w \left(\frac{2V}{r_w}\right)^2} \cos\alpha = \frac{C_1}{Re_{D_h}} \cdot \frac{r_w}{D_h} \frac{\cos\alpha}{\cos\phi} \tag{16}$$

or

$$Ri \simeq 2C_1^{3/2} \sqrt{\frac{Pr}{Gr_E}} \sqrt{\frac{A_{ct}}{A_{ch}}} \frac{r_w}{D_h} \frac{\cos\alpha}{\cos^{3/2}\phi}. \tag{17}$$

That is, Ri varies as $(Gr_E)^{-\frac{1}{2}}$ and thus as $\dot{E}^{-\frac{1}{2}}$, so increasing the heating rate reduces the stability to disturbances in the shear layer. When Ri is reduced to $O(1/4)$, multiple cells, temporal waves, or turbulence might be expected. The vertical tube, with $\cos\phi = 1$ and $\cos\alpha = 0$, would appear to be inherently unstable in this sense.

The predictions above have been developed by assuming a "long" tube, i.e., one sufficiently long that velocity and temperature fields can be considered independent of *end effects* and, therefore, fully established (idealizations 2, 4, 7, and 8). In order to examine the validity of this assumption, we can compare the situation to the entrance of a duct with forced convection and relate the common quantities. By applying the results of McEligot, Taylor, and Durst (1977), one may derive the following order-of-magnitude estimates,

$$\frac{L_{flow}}{D} \geq \frac{0.1}{4} Re_{D_h} = 0.0125 \sqrt{\frac{Gr_E A_{ct}}{C_1 Pr A_{ch}} \cos\phi} \quad \text{for friction} \tag{18}$$

and

$$\frac{L_{ht}}{D} \geq \frac{0.1}{4} Re_{D_h} Pr = 0.0125 \sqrt{\frac{Gr_E Pr}{C_1} \frac{A_{ct}}{A_{ch}} \cos\phi} \quad \text{for heat transfer} \tag{19}$$

where D represents the diameter of a circular tube, the depth of a duct, an axis of an ellipse, etc. A comparable approximation was considered by Batchelor (1954) in estimating how tall a narrow cavity must be in order to neglect end effects. One sees that the approximate development length L/D varies as $\sqrt{Gr_E}$ and, therefore, as $\sqrt{\dot{E}}$. The choice of fluid can have a substantial effect since L_{ht}/D varies as $\sqrt{Pr}$ also.

3. EXPERIMENT

The experiment was designed to examine natural circulation in a long tube of variable inclination from vertical, with heating from below, cooling at the top, and heat transfer through side walls, as might occur in a realistic geothermal application.

3.1. Experimental Apparatus and Design

In order to obtain low values of Rayleigh and Grashof numbers, as desired, one must (1) reduce the tube diameter to values less than 10 mm where it becomes impractical to insert and to locate thermocouples or flow visualization tracers carefully, or (2) reduce $\dot{E}$ to values such that temperature differences are less than a hundredth of a degree, which is impractical to measure, or (3) increase the fluid viscosity. We chose to increase the fluid viscosity by using a 6% aqueous solution of polyvinyl alcohol, resulting in viscosity about 60 times that of water.

Viscosity of the solution was measured at 25°C with a Brooks viscosimeter at several different rotation speeds. There was no significant variation in viscosity with strain rate, so it was concluded that the fluid could be considered Newtonian in this range. Temperature dependence of viscosity was taken to be the same as for a comparable fluid, VINOL V-350 (Geary, 1984). Thermal conductivity was measured over a range from 10°-60°C by the Dynatech Corp., Cambridge, Massachusetts (Brzezinski, 1984), by the guarded comparative technique in a horizontal cell heated from above. Specific gravity of VINOL V-350 was provided by Air Products Co., Allentown, Pennsylvania (Geary, 1984); it was within about 1% of that of pure water.

The heart of the apparatus was a pivoting test section constructed of Plexiglas as shown schematically in Fig. 4. Inner diameter was 1.93 in. (4.9 cm) and wall thickness was 0.25 in. (0.6 cm). The angle could be varied from vertical to ±40° from vertical. It was measured to within ±0.1° with the inclinometer feature of a Bruton "Pocket Transit."

A well-type heater of copper and electrical heating tape provided an approximately isothermal heat source at the bottom. A Solar constant voltage regulator provided ac power to a Superior Electric variable transformer that governed the electromotive force to the heating tape. The voltage across the tape was measured with a Hewlett-Packard 3456A digital voltmeter. Current was determined by

measuring the voltage across a shunt, a precision resistor, and directly with a Keithley 177 digital multimeter. Four type E thermocouples measured heater surface temperatures.

The copper cooler on top was an axisymmetric configuration with a small central circular tube forming a jet that impinged on the end. An alcohol-water solution, cooled to near 0°C by the Neslab refrigerated bath, flowed through this cooler and then through a Gilmont variable area flowmeter ("rotameter"), size 13. Circulation was accomplished by a Manostat "Varistaltic" pump, A-series. Coolant temperatures were measured at the inlet and outlet with type E thermocouples from the same batch as the internal thermocouples described below. The distance from the top of the well heater to the bottom of the cooler was 70 in. (178 cm), giving an aspect ratio of about 36. The cooler and heater were enclosed in fiber glass insulation to reduce heat losses.

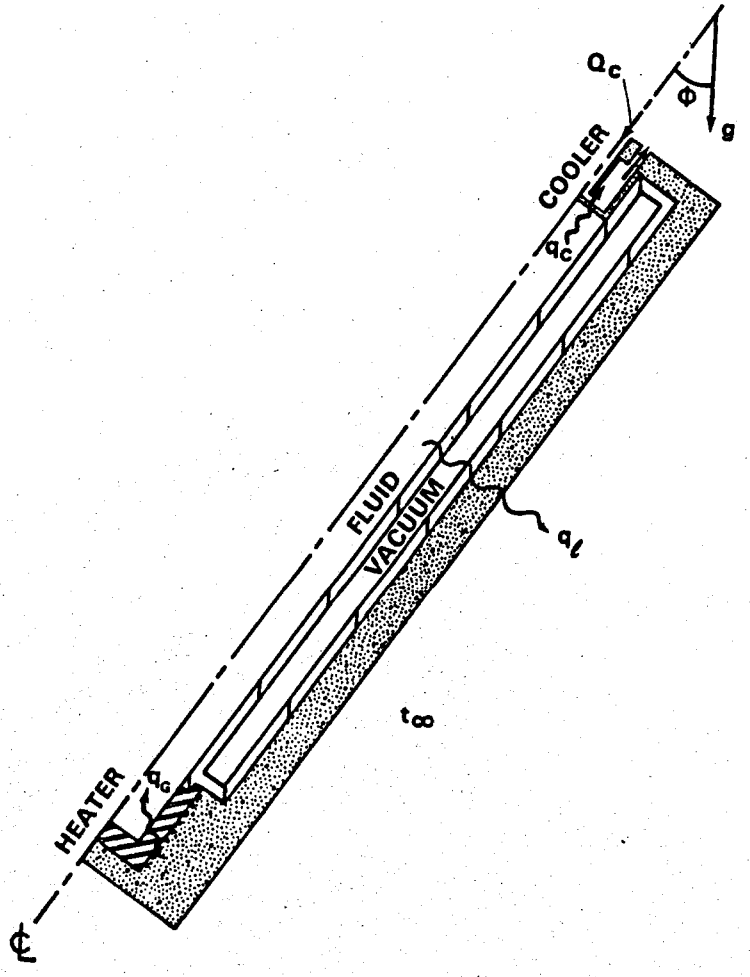

Fig. 4. Schematic diagram of apparatus.

To avoid excessive heat losses from the Plexiglas tube and still be able to visualize flow patterns and to measure velocity and temperature profiles, the test section was surrounded by another Plexiglas tube, aluminum foil, and 2 in. (5 cm) of Fiberglas insulation. Between the two Plexiglas tubes a moderate vacuum was maintained to increase the thermal resistance. Removable viewing ports were constructed in the insulation. Overall, the apparatus had a thermal time constant of about seven hours, so the viewing ports could be opened for the visual measurements for a reasonable time without excessively disturbing the thermal environment.

Calibrated chromel-constantan thermocouples, all of which were constructed from the same spool or wire, were inserted through the Plexiglas tube into the fluid. All were mounted on the vertical centerplane. One row was located about 0.5 in. (1.3 cm) from the wall along the lower surface, and a comparable row was the same distance in from the upper surface. In addition, there were five stations where three thermocouples were positioned in line radially at depths of 0.14, 0.5, and 0.8 in. (0.3, 1.3, and 2.0 cm) from the tube surface.

Three pairs of small access ports were installed through the two Plexiglas tubes and vacuum region in order to insert a thermocouple probe for radial traverses, or to inject fluid for flow visualization and velocity measurements. The ports were constructed of plastic tubing and "Swagelok" tubing connectors; at the outer end a rubber plug-type seal was held captive by the nut. The thermocouple probe or hypodermic needle containing a tracer fluid could be passed through the seal without causing any leaks.

Trace amounts of Thymol-blue were added to the fluid for flow visualization (Baker, 1966). This solution was titrated to its acid-base color change point, where it had a light yellow-brown color, by adding dilute solutions of acids or caustic sodas as necessary to adjust the pH. Then injection of a very dilute, neutrally buoyant solution of NaOH through the access ports changed the pH locally, giving a blue color, to trace the fluid motion.

3.2. Expected Conditions

Experimental parameters can be estimated in terms of the analysis of Section 2. At an inclination of 35°, fluid temperature of 100°F (38°C), and convected power of $\dot{E} = 75$ watts, approximate conditions were:

$t_h - t_c \simeq 1.2°F \simeq 0.7°C$	$Gr_E \simeq 1.3 \times 10^5$
$\frac{dt}{dx} \simeq 0.2°F/ft \simeq 0.4°C/m$	$\dot{E}/(-kA_t\frac{dt}{dx}) \simeq 2 \times 10^5$
$V \simeq 0.6$ in./sec $\simeq 1.5$ cm/sec	$Ra_{dt/dx} \simeq 240$
	$Re \simeq 3.2$
$L_{flow}/D \simeq 0.08$	$Ri \simeq 3 (\gg 1/4$, "stable")
$L_{ht}/D \simeq 27$	

As the heating rate $\dot{E}$ is reduced, Gr_E and Re decrease. Since Ri is given by

$$Ri \simeq \frac{C_1}{Re_{D_h}} \cdot \frac{r_w}{D_h} \cdot \frac{\cos\alpha}{\cos\phi}, \tag{20}$$

the single counterflow cell would be predicted to be more stable at lower heating rates. Reducing the inclination from 35° to 20° reduces Ri by about a factor of 2, so the cell would still be expected to be stable at this heating rate. For a vertical tube, the analysis of Section 2 gives $Ri = 0$, which indicates that the hypothesized single counterflow cell would be unstable to small disturbances; thus, the simplified analysis would not be expected to be valid in that limit.

3.3. Observations

Figure 5 shows a velocity profile measured with the Thymol-blue tracer technique for 31° inclination and input heating of about 10 watts. One sees the expected profile: a descending plume on one side and a rising plume on the other. The Rayleigh number for this flow was estimated to be 30, one-seventh the critical value for vertical tubes; hence it is clear that, as expected, inclined wells are more subject to natural convection than vertical wells.

Time-motion tracer studies for this flow showed that even the maximum velocities were small, of the order of 1 mm/sec. Thus, although convection did occur, it was weak. Further evidence of this weakness is provided in Fig. 6, which shows the disturbing effect that the small thermocouple wires had upon the flow streamlines. Occasionally this disturbance became so strong that it could break up the single cell convection pattern and produce multiple cells, each of which were only a few diameters long, quite similar to Diment's (1967) observations in actual wells.

Measurements were obtained at various heating rates and tube inclinations. The maximum angle was 35° from the vertical; this was also the inclination most frequently used. Nine experimental

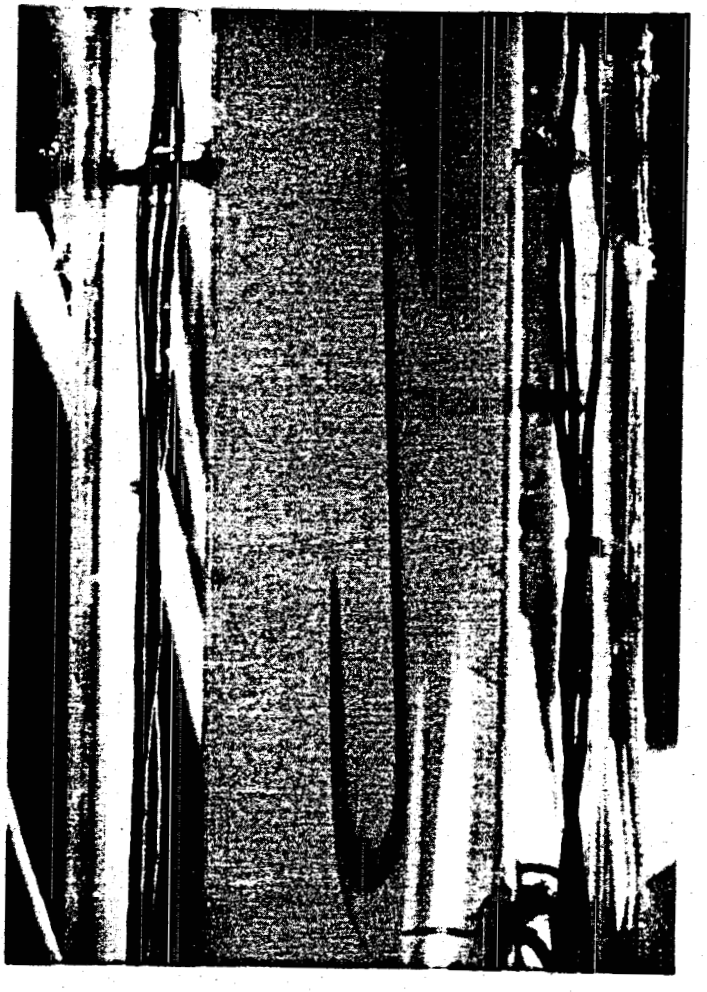

Fig. 5. Velocity profile with low heating rate in inclined tube, $\phi = 31°$, $q_G = 10$ W.

runs were conducted. The most extensive data available are transient temperatures recorded via the thermocouples in the fluid.

Typical transient response is demonstrated in Fig. 7. Inclination was 35° and heating rate was 73 watts, the highest used. Initially, the fluid was nearly isothermal at 34°C (93°F). After one-half hour of heating the temperature distribution had assumed the shape shown in the second subfigure. With the exception of minor details, this shape was maintained for the next 4 hours while the temperature level gradually increased.

The time constant, and therefore the rate of temperature increase, is dominated by the thermal resistance of the insulation and is slow. However, it appears that a quasi-steady temperature distribution was reached relatively quickly. Presumably this distribution corresponded to a near steady flow pattern. For this inclination (35°), the (near) "wall" temperatures show the warm fluid to be

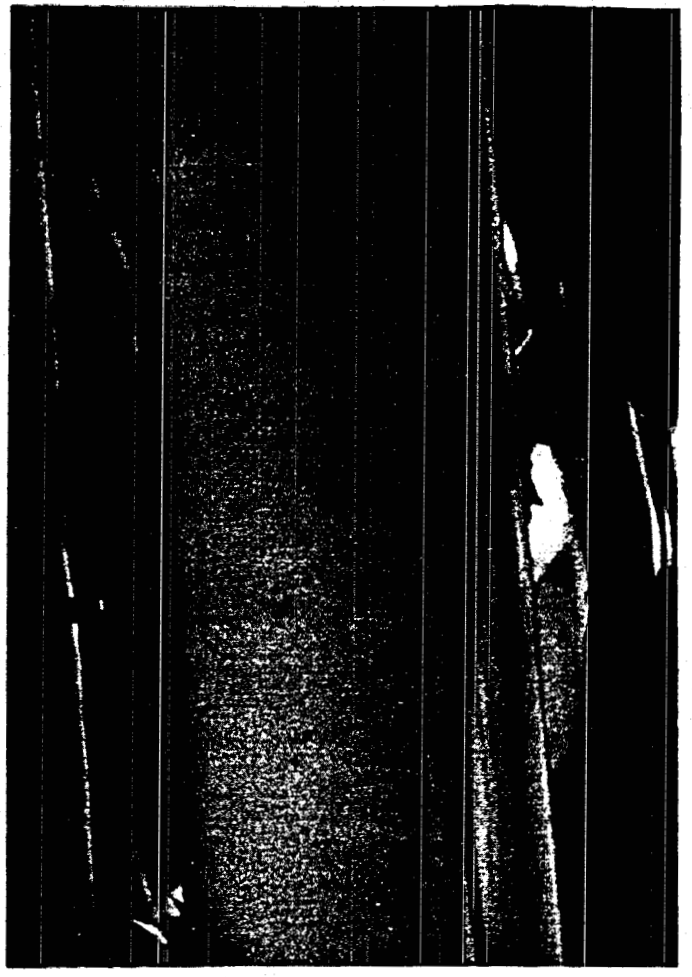

Fig. 6. Indication of flow disturbance by thermocouple during weak convection, $\phi = 31°$, $q_G = 10$ W.

rising along the upper side and cool fluid to be descending on the lower. There is a slight decrease in the axial direction, but near the central midplane the temperatures seem near isothermal. These observations correspond to a long, single recirculating cell along the tube. However, the thermocouple readings at the top near the cooler may indicate a small cell with circulation in the opposite direction. Details of additional experimental runs are included later in Section 5, Comparison of Experiments with Predictions.

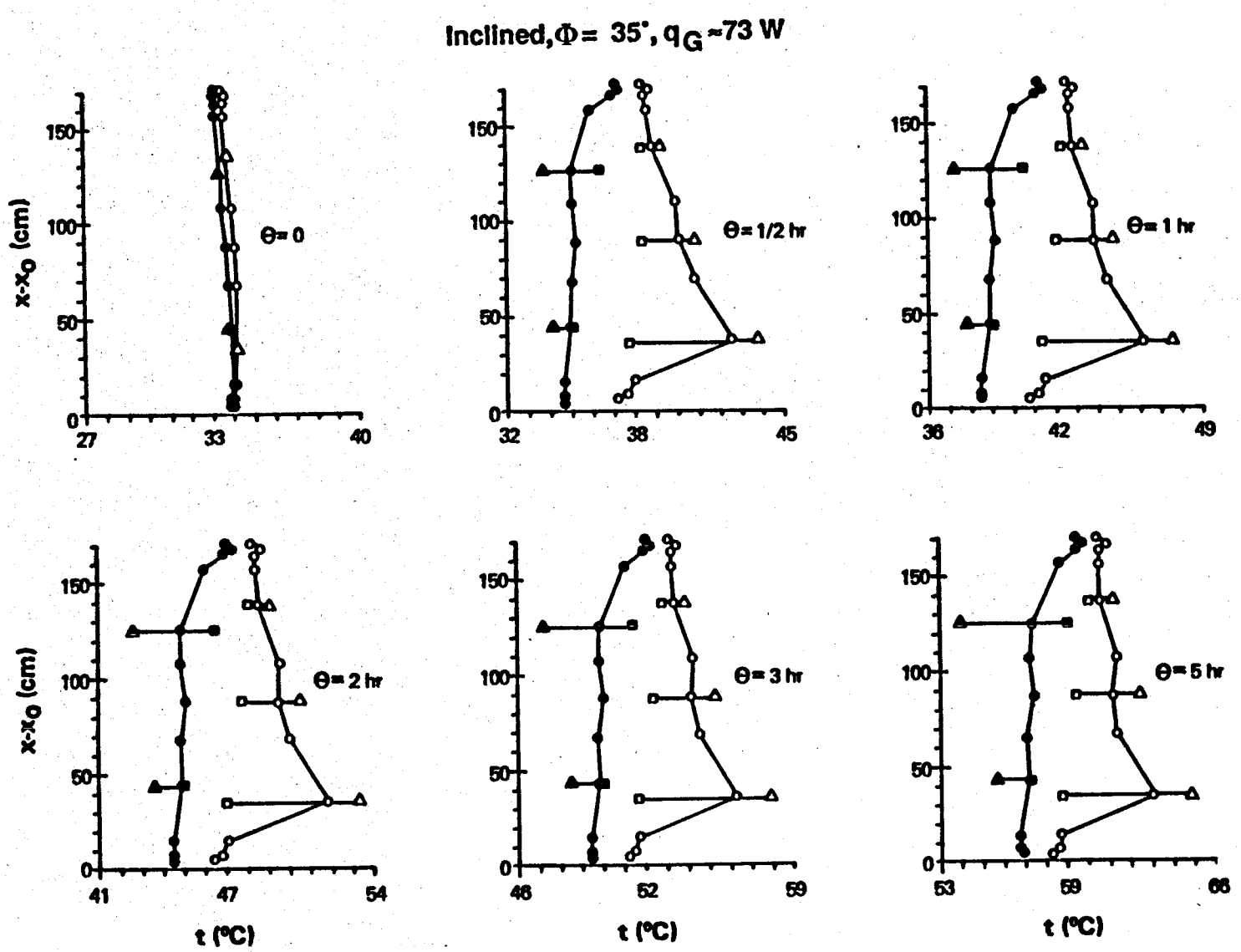

Fig. 7. Transient response during heating run. (Thermocouples: Δ = "near" wall, 0 = intermediate, ▫ = "near" center, r/r_w = 0.85, 0.48, 0.17, respectively, open = upper, closed = lower).

4. NUMERICAL PREDICTIONS

4.1. Choosing the Code and Model

A variety of computer programs is available for the solution of general fluid mechanics and heat-transfer problems (Johnson and Torok, 1985). In order to simulate transient, three-dimensional flow with variable properties, we chose TEMPEST (Transient Energy, Momentum, and Pressure Equation Solution in Three dimensions), developed by Trent *et al.* (1983). For code assessment and validation, predictions have been compared with experimental data, analytical solutions, and predictions of other codes in a separate report by Eyler *et al.* (1983). TEMPEST provides finite-difference solutions to the equations governing mass, momentum, and energy for incompressible single-phase flows with small density variations (Boussinesq approximation). The finite-difference approach for the fluid-flow solution is similar to the SMAC method (Amsden and Harlow, 1970) whereby the momentum and energy equations are solved explicitly, and the continuity/pressure solution is obtained implicitly. Additional features of importance for the present application include treatment of coupled solid and fluid regions, capability to specify heat transfer coefficients for individual surfaces, cylindrical coordinates, arbitrary orientation relative to gravity and variable grid spacing.

In order to allow for most features of the experimental apparatus, a three-dimensional, circular coordinate system was chosen with multiple regions. However, to reduce computer time and storage requirements, a very coarse grid was used. Including dummy nodes required by the calculation technique, the grid consisted of 6 nodes in the radial direction and 12 axially. The circumferential direction was represented by 8 nodes on 45° planes plus cyclical (or repeating) nodes at each end, for a total of 10. Thus, the three-dimensional geometry was modeled by 720 nodes overall. Spacing was variable in the radial and axial directions and uniform circumferentially. The electrical resistance heating was modeled by volumetric energy generation sources in appropriate cells. The variable spacing was applied to concentrate nodes near the cooler end where the largest temperature gradients were expected. Large aspect ratios $\Delta L/D$ of the axial spacing along most of the tube probably prevent identifying cellular structures that could occur at some inclination angles and heating rates.

4.2. Testing The Model

In addition to the verification studies conducted by Eyler *et al.* (1983), a few tests of the TEMPEST code were applied for limiting situations related to the geometry of the inclined natural convection experiment. The general features of the experimental apparatus were approximated by the numerical grid specified, then quantities were adjusted to represent simple idealized cases for which closed-form solutions are available. It is recognized that the grid is so coarse that the flow field is likely grid-dependent, possibly missing details such as corner eddies. However, since the flow is considered to be laminar in the range studied, the heat transfer perpendicular to the streamlines is by molecular conduction. The full three-dimensional code was tested by comparison with the following limiting analyses:

- steady, one-dimensional, axial conduction
- transient approach to steady state with one-dimensional axial conduction;
- transient, one-dimensional radial conduction; and
- transient approach to one-dimensional fin (extended surface) solution.

The results were reasonable for the coarse grid used and were as expected.

4.3. Time Scales

Because TEMPEST solves the governing equations via an explicit numerical technique, there is a large disparity between the various time scales occurring in the calculation. In attempting to handle some of the regions where large gradients were expected while using a coarse grid, some cell aspect ratios became large. For example, the ratio of the largest-to-smallest spacing was $60/0.65 = 92$. For insight, it is convenient to consider the criteria that would apply if the problem were one-dimensional (Incropera and deWitt, 1981). For the energy equation, an explicit calculation would require a time step of

$$\Delta\theta \leq \frac{1}{2}\frac{(\Delta x)^2}{\alpha}. \tag{21}$$

For the fluid, the time step could be about 0.05 hr $\simeq$ 3 min $\simeq$ 170 sec. A constraint for the momentum equation would be

$$\Delta\theta \leq \frac{1}{2}\frac{(\Delta x)^2}{\nu} = \frac{1}{2}\frac{(\Delta x)^2}{Pr \cdot \alpha} \tag{22}$$

where Pr is the Prandtl number, $c_p\mu/k$. For the viscous fluid of the experiment, the kinematic viscosity, ν, is about 1.56 ft^2/hr (0.145 m^2/hr), so $Pr \simeq 330$. Thus, the maximum time step for of the momentum equation would be of the order of 1.5×10^{-4} hr or 0.5 sec. With an explicit solution of the momentum equation, the number of time steps to approach a steady fluid-flow solution would be

$$n = \frac{\theta}{\Delta\theta} \geq \left(\frac{r_w}{\Delta x_{\min}}\right)^2 \tag{23}$$

where $\Delta x_{\min}$ represents the minimum value of Δr or Δz and θ is the approximate time for response to within about five per cent for an imposed change. On the other hand, to approach a steady thermal flow in the fluid would require

$$n = \frac{\theta}{\Delta\theta} \geq Pr\left(\frac{r_w}{\Delta x_{\min}}\right)^2. \tag{24}$$

As an example, for the coarse mesh used, with $\Delta x_{\min} \simeq r_w/4$, and the viscous fluid used in the experiment, about 16 time steps would be required for fluid response and over 5000 for thermal! (Since the thermal distribution drives the fluid through buoyancy, it would be expected that the latter would determine the required calculation time.) With time steps of 1.5×10^{-4} hr, thermal response times of about three-fourths hour are predicted.

These estimates do not include the response of the insulation, which is estimated to introduce a time constant of about 7 hours. These values agree qualitatively with experimental observations: a quasi-steady distribution appeared in about one-half hour, but one-half to one day was necessary before the temperature level could be considered steady.

Calculations were conducted to obtain steady-state results for the operating conditions of four experiments. These experiments spanned the range of inclination angles and heating rates considered, $0 \leq \phi \leq 35$ and $12 \leq \dot{E} \leq 73$ watts.

Despite the a very coarse mesh, transient calculations were slow. For example, even with continuous readjustment of the time step, it was about 2×10^{-5} hr, so 5000 steps represented 0.1 hr or 6 minutes of simulated time. The total execution time was about 460 seconds or nearly 8 minutes on the CDC 7600. That is, simulated time and computer time were nearly the same. Therefore, an alternate technique of estimating the steady distributions was used.

TEMPEST includes an option to expedite the approach steady state. It uses an iterative solution of the steady-state energy equation (i.e., storage term suppressed) at each time step using the most recent calculations of the more rapidly developing velocity and pressure fields. Thus, this approach can accelerate the determination of the steady flow field if the changes from step to step are not too large. One key to this procedure seemed to be ensuring a reasonably well converged solution of the pressure field at each step. The procedure that evolved was to apply this option for the first 100 time steps to approximate the steady state fields and then to calculate 5000 to 20,000 steps as a simple transient so the details could settle. The initial condition at the first step was taken as the approximate temperature level of the experiment being simulated.

5. COMPARISON OF EXPERIMENTS WITH PREDICTIONS

There are two interrelated aspects of the comparison. One is the general agreement with the trends predicted by the numerical analysis (and to some extent the simple analysis) for the temperature distribution along most of the length of the apparatus simulating the wellbore. Secondly, in the experiment the thermal resistance to the cooling end plate is of the same order-of-magnitude as the resistance through the walls; since the surface area of the end is considerably smaller. The largest temperature difference is between the fluid and the end. In this section we address the general comparison first and then concentrate on the treatment of the end region. These comparisons are for resulting steady conditions.

5.1. Temperature Profiles

Comparisons of the axial temperature profiles predicted and those measured with the immersed thermocouples are presented in Fig. 8 for steady state. Solid lines represent the predictions using the coarse grid described earlier and the circular symbols depict the data, all at $r/r_w = 0.48$, the middle point along a radius in the fluid. For the inclined tube the higher temperatures correspond to the upper sector of the cross section where the heated fluid rises, while the lower temperatures correspond to the lower sector. Data are not presented in this representation for the experiment at a heating rate of 73 watts since steady-state conditions were not attained. During the measurements it appeared that temperatures in the well heater were nearing the boiling temperature of water at Los Alamos elevation,

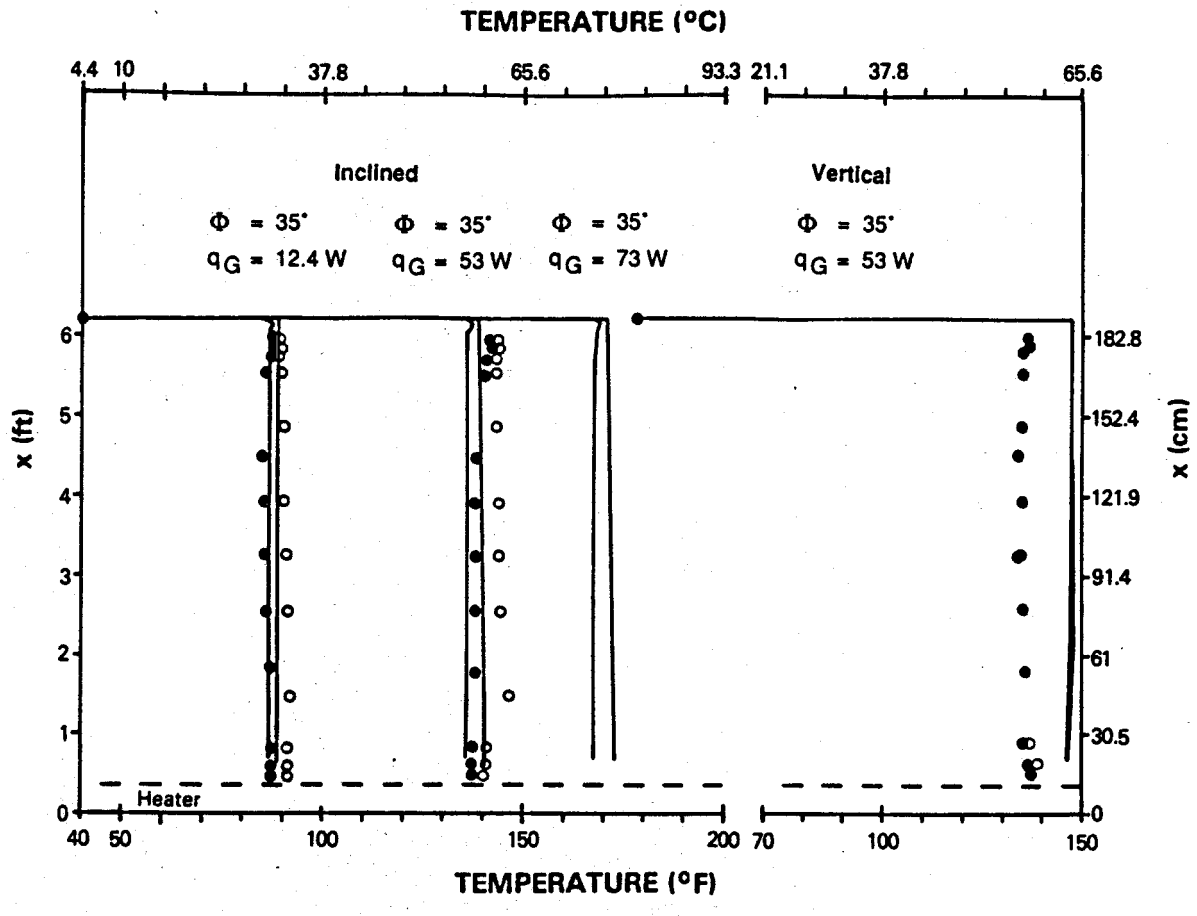

Fig. 8. Steady-state predictions compared with measurements.

7000 ft (2100 m) MSL, so the voltage across the resistance heater was reduced twice. The final steady condition was reached with 53 watts as shown.

For the predictions presented for the vertical case, the initial conditions were taken as uniform temperature at 135°F (57.2°C), the approximate average temperature of the preceding run, and velocities set at zero.

Agreement is remarkable despite some differences in details. It can be taken as partial confirmation of the usefulness of the computer code and of aspects of the simple analysis.

Along the length of the tube, the temperature variation is very slight as predicted by the simple analysis for inclined tubes. Thus, the temperature level is determined by the energy generation rate from the electrical heater, the cooler temperature at the top end and the thermal resistances to heat loss through the insulation and convective heat transfer to the cooler. The cooler acts as the thermal reservoir providing the datum or reference temperature for the experiment.

5.2. End Region Results

Because the heat loss coefficient of the apparatus was calibrated by a cooling experiment and then was adopted for the calculations, the prediction of the heat-transfer loss through the tube walls, vacuum jacket, and insulation can be expected to be reasonably good. In fact, if the heat transfer to the cooling end were small, this radial heat loss would dominate in determining the fluid temperature level and these comparisons would not be meaningful tests of the predictions. This is not the situation in the present study. The heat loss through the insulation and heat transfer to the cooler are estimated to be of the same order of magnitude, ranging from $(q_\ell/q_c) = 0.6$ to 1.2 for the data shown.

The approximate agreement of temperature levels demonstrates that, despite the coarse mesh, the numerical prediction of the velocity and temperature distributions in the fluid provides a good estimate of the thermal resistance at the cooled upper end. An average Nusselt number can be calculated for the cooled end as

$$Nu_c = \frac{h_c D}{k_c} = \frac{4q_c}{\pi D k_c (t_f - t_c)}, \tag{25}$$

where t_f could be taken as a fluid temperature in the core of the tube, extrapolated to $z = L$. Since $t(z)$ is almost isothermal at the aspect ratio of this apparatus, an average temperature would be a fair approximation for t_f. Whether t_c, t_f, or an intermediate (film) temperature is most useful for evaluating properties in correlating the data is a question for further research. In the present study the variation of $k(t)$ is slight (and uncertain) (Brzezinski, 1984).

From numerical predictions, the average Nusselt number usually would be approximated as

$$Nu_c = \frac{q''}{(t_f - t_c)}\frac{D}{k_c} \simeq -\frac{t_N - t_{N-1}}{t_f - t_c}\frac{D}{Z_N - Z_{N-1}} \tag{26}$$

(where N represents a node on the cooled surface) or a higher order version. However, the grid is too coarse for representing $\partial t/\partial z$ by $\Delta t/\Delta z$, so Nu_c was predicted via the energy balance ($q_c = q_G - q_L$) as in the data reduction from the experiment.

The appropriate independent parameter for correlating the heat transfer at the cooled end would be a Rayleigh number or Grashof number, based on heat-transfer rate or temperature difference. Provided the aspect ratio, L/D, is long enough, one would expect the result to be independent of aspect ratio. The Rayleigh number for the enclosed end can be defined as

$$Ra_c = Gr_c \cdot Pr = \left(\frac{\rho^2 g \beta D^4 (q_c''/k)}{\mu^2}\right) \cdot \left(\frac{c_p \mu}{k}\right). \tag{27}$$

Gr_c relates to Gr_E, defined via Eqs. (13) and (10) as

$$\frac{Gr_c}{Gr_E} = \left(\frac{D}{D_h}\right)^4 = O(2^4). \tag{28}$$

Again, the question arises concerning which temperature(s) to use in evaluating the fluid properties. In the typical idealized problem for the end of a tube, the known conditions would probably be a) t_f and t_c or b) q_c'' and t_f, plus $\rho(t)$ and $\mu(t)$ and the geometry and inclination. To examine the influence of fluid property selection, with the present data the properties were evaluated at two temperatures t_c and $t_f \simeq t_{avg}$. Predictions were calculated for laminar flow with constant properties, other than in the Boussinesq approximation, with 100°F $\simeq$ 38°C taken as the fluid temperature. These measurements and predictions of $Nu_c(Ra_c)$ are compared in Fig. 9 for the three steady-state results. The solid line represents the predicted trend based on the two sets of calculations at an angle of 35°, while the dashed line below shows the prediction for the vertical tube, based on a single calculation. Circular symbols show the measurements when t_c is used to evaluate fluid properties, and squares are for Nu_c and Ra_c based on an approximate average fluid temperature. The solid symbols are for the vertical tube, and the open ones are for the angle of 35°.

One sees better agreement when Ra_c is based on properties evaluated in the fluid away from the cooled surface; these properties would be comparable to the freestream in an external flow. Since Ra_c (or Ra_E) can be considered to be the driving parameter for the natural circulation, it may be reasonable to expect its value away from the surface to determine the strength of the recirculating flow field, which serves approximately as a boundary condition for the heat transfer to the end region.

While the trend of increase in Nu_c with increase in heating rate (Ra_c) is seen in both the predictions and data for the 35° angle, the variation with angle differs. In the predictions Nu_c is reduced about 10% by changing the angle from 35° to vertical. On the other hand, the measurements show an increase of 15 to 20% percent. Since the calculations were for laminar flow, this observation may be another indication that the flow in the vertical orientation is unstable, turbulent, or involves more recirculating cells than predicted. It should be recalled that, in the simple analysis, application of Hines (1971) treatment of nonhorizontal shear layers led to

$$Ri \sim \frac{\cos(\pi/2 - \phi)}{\cos^{3/2}\phi}, \tag{29}$$

which is zero for vertical tubes. Values of R_i less than one-fourth are believed to be unstable. This result implies that countercurrent flow consisting of a single, long cell is inherently unstable in the

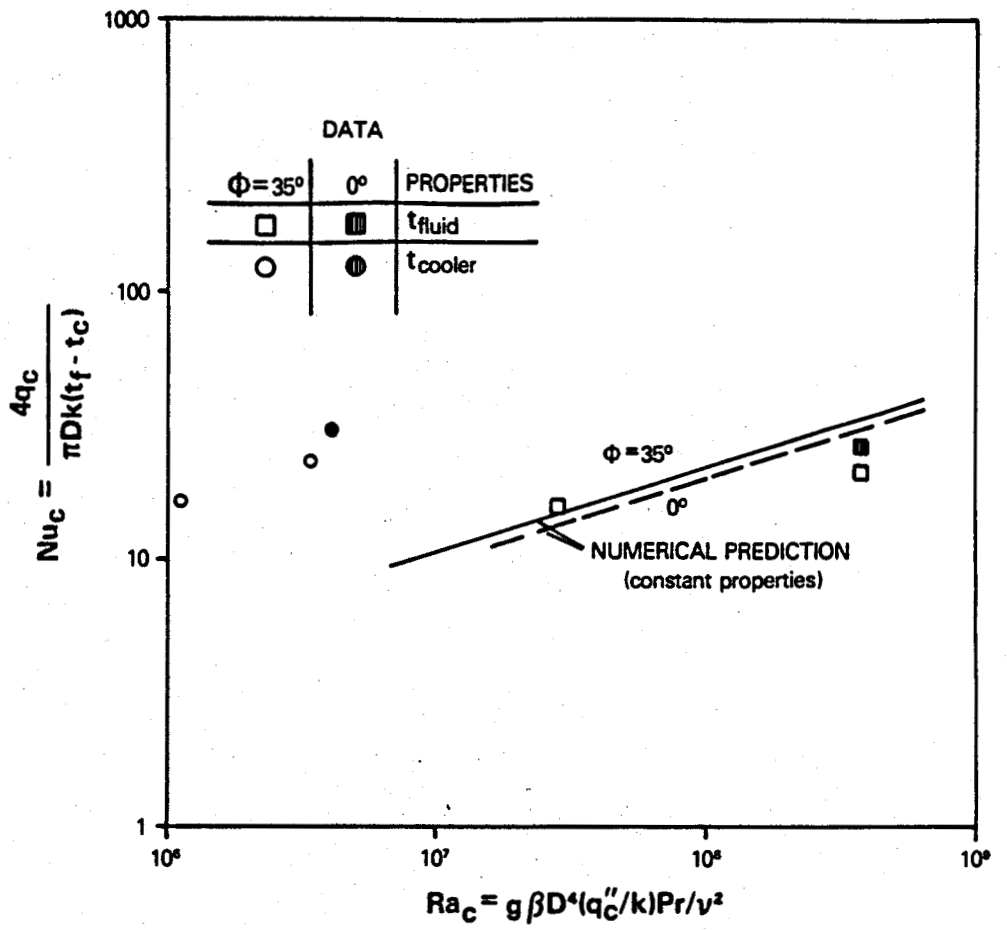

Fig. 9. Convective heat transfer at cooled end. Measurements compared with numerical predictions.

vertical configuration. A turbulent or unstable flow would be expected to provide better transport of thermal energy to the end surface than laminar flow and, therefore, increase the Nusselt number. Further calculations, and perhaps additional experiments, are necessary to resolve these aspects of the problem and are beyond the present scope of the work.

6. CONCLUDING REMARKS

Natural convection in inclined tubes with heat loss through the wall was studied analytically and numerically, and the predictions were compared with measurements in a comparable experiment. Although the results should be considered primarily qualitative rather than quantitative, useful insight evolved.

The simple analysis predicted that, under the idealizations imposed, the effects of increasing the heating rate $\dot{E}$ are

- to increase the induced flow rate as $\sqrt{\dot{E}}$,
- to increase $(t_h - t_c)$ as $\sqrt{\dot{E}}$, and
- to leave dt/dx constant.

Consequently, away from ends, the Rayleigh number based on streamwise temperature gradient is predicted to be a function of geometry and inclination only, varying as $1/\cos\phi$. The stability of the hypothesized countercurrent flow, consisting of a single, long cellular pattern, was represented in terms of a Richardson number; this number is a function of inclination and varies as $1/\sqrt{\dot{E}}$. Small values indicate potential instability, so increasing the heating rate or reducing the angle toward the vertical tends to make the single cell unstable to small disturbances.

Numerical predictions were conducted for comparison with four experiments over a range of heating rates from 12 to 73 watts and inclination angles from vertical to 35°. Comparison with experiments showed good agreement of temperatures for the maximum inclination of 35° and slightly poorer agreement for the other limit, a vertical tube. Trends of temperature and Nusselt number with heating rate or Rayleigh number were reasonable, but the variation of (cooled) end Nusselt number with inclination was opposite to that observed in the experiment. Further study is needed to understand this latter observation, but the measured increase in Nusselt number could be considered to be consistent with simple stability theory coupled with the predictions of a simple analysis.

ACKNOWLEDGMENTS

This work was supported by the U.S. Department of Energy Geothermal Energy Program. George Zyvoloski of Los Alamos National Laboratory provided the support necessary to use the Laboratory's CDC 7600; Loren Eyler of Battelle Pacific Northwest Laboratory made the TEMPEST code available and provided guidance in its use.

REFERENCES

Amsden, A. A., and F. H. Harlow, 1970. *J. Comput. Phys.*, **6**, pp. 322-325.

Baker, D. J., 1966. *J. Fluid Mech.*, **26**, pp. 573-575.

Batchelor, G. K., 1954. *Q. Appl. Math.*, **12**, pp. 209-233.

Brzezinski, A. J., 1984. Dynatech Company letter LOS-1 of 10 July 1984.

Buchberg, H., I. Catton, and D. K. Edwards, 1976. *J. Heat Transfer*, **98**, pp. 182-188.

Catton, I., 1978. *Proc., 6th Int. Heat Transfer Conf.*, Toronto, **2**, pp. 13-31.

Catton, I., and D. K. Edwards, 1967. *J. Heat Transfer*, **89**, pp. 295-299.

Charlson, G. S., and R. L. Sani, 1970 *Int. J. Heat Mass Transfer*, **13**, pp. 1479-1496.

Charlson, G. S., and R. L. Sani, 1971. *Int. J. Heat Mass Transfer*, **14**, pp. 2157-2160.

Combarnous, M., 1978. Natural convection in porous media and geothermal systems. *Proc., 6th Int. Heat Transfer Conf.*, Toronto.

Diment, W. H., 1967. *Geophysics*, **32**, pp. 720-726.

Donaldson, I. G., 1961. *Aust. J. Phys.*, **14**, pp. 529-539.

Donaldson, I. G., 1968. *Proc., 3rd Australasian Conf. Hydraulics and Fluid Mech.*, pp. 200-204.

Donaldson, I. G., 1970. *Geothermics* – Spec. Issue **2**, pp. 649-654.

Edwards, D. K., 1969. *J. Heat Transfer*, **91**, pp. 145-150.

Edwards, D. K., and I. Catton, 1969. *Int. J. Heat Mass Transfer*, **12**, pp. 23-30.

Einarsson, T., 1942. *Rit. Visind. Isl.*, **26**, pp. 1-92 (in German).

el Sherbiny, S. M., G. D. Raithby, and K. G. T. Hollands, 1982. *J. Heat Transfer*, **104**, pp. 96-102.

Eyler, L. L., D. S. Trent, and M. J. Budden, 1983. Battelle Pacific Northwest Laboratory technical report PNL-4348 Vol. II, UC 79T.

Geary, M., 1984. Personal communication, Air Products Company.

Gretener, P. E., 1967. *Geophysics*, **32**, pp. 727-738.

Hales, A. L., 1937. *R. Astrophys. Soc. Geophys. Suppl.*, **4**, pp. 122-131.

Hartnett, J. P., W. E. Welsh, and F. W. Larsen, 1959. *Chem. Eng. Prog., Symp. Ser., Nucl. Eng.*, **55**, p. 85.

Hasegawa, S., K. Nishikawa, and K. Yamagata, 1963. *Bull. Japan Soc. Mech. Eng.*, **6**, pp. 230-250.

Heitz, W. L., and J. W. Westwater, 1971. *J. Heat Transfer*, **93**, pp. 188-196.

Hess, S. L., 1959. *Introduction to Theoretical Meteorology.* New York: Holt, Rinehart, and Winston.

Hines, C. O., 1971. *Q. J. R. Meteorol. Soc.*, **97**, pp. 429-439.

Incropera, F. P., and D. P. deWitt, 1981. *Fundamentals of Heat Transfer.* New York: Wiley.

Japiske, D., 1973. *Adv. Heat Transfer*, **9**, pp. 1-111.

Johnson, A. E., and D. Torok, 1985. *Comput. Mech. Eng.*, pp. 41-45 (July 1985).

Kays, W. M., and A. LLondon, 1964. *Compact Heat Exchangers*, 2nd ed. New York: McGraw-Hill.

Kimura, S., and A. Bejan, 1980a. *Int. J. Heat Mass Transfer*, **23**, pp. 1117-1126.

Kimura, S., and A. Bejan, 1980b. Wärme and Stoffübertragung, **14**, pp. 269-280.

Leslie, F. M., 1959. *J. Fluid Mech.*, **7**, p. 115.

Lighthill, M. J., 1953. *Q. J. Mech. Appl. Math.*, **6**, pp. 398-439.

Martin, B. W., 1959. *Proc., Inst. Mech. Eng.*, **173**, pp. 761-778.

McEligot, D. M., D. A. Denbow, and H. D. Murphy, 1990. *Transient natural convection in heated inclined tubes.* Los Alamo National Laboratory report LA-11813-MS.

McEligot, D. M., M. F. Taylor, and F. Durst, 1977. *Int. J. Heat Mass Transfer*, **20**, pp. 475-486.

Mertol, A., W. Place, T. Webster, and R. Greif, 1981. *Sol. Energy*, **27**, pp. 367-386.

Olson, J. M., and F. Rosenberger, 1979. *J. Fluid Mech.*, **92**, pp. 609-629 and 631-642.

Ostrach, S., 1982. *Proc., 7th Int. Heat Transfer Conf.*, München.

Ostrach, S., and P. R. Thornton, 1958. *Trans., ASME*, **80**, p. 363.

Ostroumov, G. A., 1952. NACA technical memorandum 1407 (1958).

Rowley, J. C., and R. S. Carden, 1982. Los Alamos National Laboratory report LA-9512-HDR.

Schlichting, H., 1968. *Boundary Layer Theory.* New York: McGraw-Hill.

Smith, M. C., G. J. Nunz, and G. M. Ponder, 1983. Los Alamos National Laboratory report LA-9780-HDR.

Trefethen, L. M., 1970. *Proc., 4th Int. Heat Transfer Conf.*, Paper NC 2.12, Versailles.

Trent, D. S., L. L. Eyler, and M. J. Budden, 1983. Battelle Pacific Northwest Laboratory technical report PNL-4348, Vol I, UC-79T, Rev. 1.

Verhoeven, J. D., 1969. *Phys. Fluids*, **12**, pp. 1733-1740.

Zvirin, Y., A. Shitzer, and G. Grossman, 1977. *Int. J. Heat Mass Transfer*, **20**, pp. 997-999.